# Supporting Information

## IN SITU-DEVELOPMENT OF A 3D Cu-$CeO_2$ CATALYST SELECTIVE IN THE ELECTROCATALYTIC HYDROGENATION OF BIOMASS FURANIC COMPOUNDS

Giancosimo Sanghez de Luna,[1] Patrick Zeller,[2,3] Eylül Öztuna,[2,3] Francesco Maluta,[1,4] Andrea Canciani,[1,4] Francesca Ospitali,[1] Phuoc H. Ho,[1] Alessandro Paglianti,[1] Axel Knop-Gericke,[2,5] Giuseppe Fornasari,[1,4] Juan J. Velasco-Vélez,[2,5,6]** Patricia Benito[1,4]*

[1] Department of Industrial Chemistry "Toso Montanari", Università di Bologna, Viale Risorgimento 4, 40136, Bologna, Italy

[2] Fritz-Haber-Institut der Max-Planck-Gesellschaft, Faradayweg 4-6, 14195 Berlin, Germany

[3] Helmholtz-Zentrum Berlin für Materialien und Energie GmbH, BESSY II, Albert-Einstein-Straße 15, 12489 Berlin, Germany

[4] Center for Chemical Catalysis – C3, Alma Mater Studiorum – Università di Bologna, Viale Risorgimento 4, 40136, Bologna, Italy

[5] Max Planck Institute for Chemical Energy Conversion, Heterogeneous Reactions, Stiftstrasse 34-36, 45470 Mülheim, Germany

[6] ALBA Synchrotron Light Source, 08290 Cerdanyola del Vallés (Barcelona), Spain

* patricia.benito3@unibo.it

** jvelasco@cells.es

## 1. Experimental part

### 1.1.Materials

Cu foam panels were supplied by Alantum. Chemicals used were sodium hydroxide (≥98%, Sigma-Aldrich), cerium nitrate (99.5%, Sigma-Aldrich), boric acid (≥99.5%, Sigma-Aldrich), and 5-hydroxymethylfurfural (99%, AVA Biochem). 2,5-bis(hydroxymethyl)furan (Toronto Research Chemicals) was used as standard for High Performance Liquid Chromatography (HPLC) analysis. All chemicals were used without further purification. Ultrapure water, UPW, (18 MΩ cm) was used for the preparation of all aqueous solutions.

### 1.2.Synthesis of Catalyst

Cu foams were cut from 450 μm cell size foam panels of 1.6 mm thickness into pieces of 10 mm x 10 mm (geometric surface area 2.64 $cm^2$). Before the electrodeposition of $CeO_2$, the foams were washed with 2-propanol, UPW, 1 M HCl for 5 min to remove surface oxides, and UPW to remove HCl. The foams were coated by electrodeposition in a home-made double compartment three-electrode cell controlled by a potentiostat/galvanostat Metrohm Autolab PGSTAT204, equipped with NOVA software as reported elsewhere [S1]. A Pt coil and a saturated calomel electrode (SCE) were used as counter and reference electrode (C.E. and R.E.), respectively. The working electrode (W.E.) was the Cu foam and it was assembled by a two-pronged Pt electrical contact. The working and counter electrode compartments were separated by a glass frit tube. The R.E. was in electrolytic contact with the main compartment *via* a Luggin capillary placed 1 mm close to the surface of the foam cylinder. The electrodepositions were performed in two electrolytes, circulating at a flow rate of 2 mL $min^{-1}$, modifying the deposition parameters to obtain different coating morphologies [S1]: i) 0.15 M $Ce(NO_3)_3$, -0.9 V vs SCE (-0.3605 vs RHE) for 100 s; ii) 0.10 M $Ce(NO_3)_3$, -1.1 V vs SCE (-0.5605 vs RHE) for 200 s. All potentials were reported vs SCE and RHE (V vs RHE = V vs SCE + 0.244V + 0.0591pH). After electrodeposition, the coated foams were thoroughly washed with distilled water and dried at 40 ºC for 12 h.

### 1.3.Characterization techniques

X-ray diffraction (XRD) analysis was carried out on the coated foam specimens using a PANalytical X'Pert diffractometer equipped with a copper anode ($\lambda_{mean}$ = 0.15418 nm) and a fast X'Celerator detector. The diffractogram was collected over a 2θ range from 3 to 80° with a step size of 0.067° and counting time per step 60.95 s.

The surface morphology of the foam electrodes was examined by Field Emission Scanning Electron Microscopy/Energy Dispersive Spectroscopy (FE-SEM/EDS) analyses were performed in a ZEISS Leo 1530 equipped with an INCA EDS microanalysis and INCA Microanalysis Suite Software (Oxford Instruments Analytical). The accelerating voltage was 10 kV and the EDS spectra were collected during a period of 60 s. The thickness of the coating was estimated from regions where some cracks are developed.

Transmission electron microscopy characterization was carried out by a TEM/STEM FEI TECNAI F20 microscope at 200 keV, equipped with an EDS analyzer. The coating was scratched from the foam and suspended in ethanol under ultrasounds. The suspension was subsequently deposited on a holey carbon film supported by an Au grid and dried at 100 °C. Particle size distribution was processed considering around 150 particles.

Micro-Raman spectra were measured using a Renishaw Raman Invia spectrometer configured with a Leica DMLM microscope. An $Ar^+$ laser source ($\lambda = 514.5$ nm, $P_{out} = 30$ mW, considering the decrease in power due to the plasma filter) was employed, setting the laser power by 10 % of the source and accumulating 4 individual spectra, for each measurement, with an acquisition time of 10 s.

Inductively Coupled plasma atomic emission spectroscopy (ICP-AES) analyses were performed using an Agilent Technologies 4210MP-AES instrument. The analysis of the solutions after HMF electrolysis was carried out to identify (not quantify) Ce and Cu. The emissions at 446.0 nm for Ce and 324.7 nm for Cu were evaluated.

The relative conductivity of the electrocatalysts was measured with the ITS 2000 ERT instrumentation (Industrial Tomography Systems Ltd), as done for other solid-liquid systems [S2]. A cylindrical test tube of diameter 20 mm was equipped with 16 circular stainless-steel electrodes of diameter equal to 2 mm, equally spaced along the circumference of the tube inner walls. Coaxial cables connected the electrodes to the Data Acquisition System (DAS) [S3]. The tested electrocatalysts were placed in the tube which was filled with a demineralized water-NaCl solution. The experiments were performed by adjusting the conductivity of the water solution where the electrode was immersed so that the immersion of an electrode, made of the bare Cu foam, did not appreciably change the conductivity inside the probe. In the following, the experimental results will be shown giving the mean values of the dimensionless conductivity, computed as the ratio between the mean conductivity measured when the tested electrocatalysts were placed in the test tube and the conductivity measured when the test tube was filled with the NaCl solution. In this way, the mean value of the dimensionless conductivity, with the Cu foam was close to 1. Values of the dimensionless

conductivity larger than 1 indicate a conductivity of the tested electrocatalyst higher than the Cu foam, while lower values imply lower conductivities.

### 1.4.Electrocatalytic tests

Electrochemical measurements were controlled by a potentiostat/galvanostat Metrohm Autolab PGSTAT204, equipped with NOVA software; Cu wires were attached to the electrocatalysts to enable connection to the potentiostat. A three-electrode three-compartment cell, separated by glass frits, was used to perform all the electrochemical measurements as reported elsewhere [S4] and shown below. Working electrodes were the electrocatalysts, placed in the central compartment, with the reference electrode (SCE) put in electrolytic contact via a Luggin capillary. Counter electrodes were Pt wires, placed in the side compartments at a distance of ca 5 cm from the working electrode. Catholytes were 25 mL of 0.5 M borate buffer aqueous solution (pH 9.2) with and without HMF 0.02, 0.05 and 0.10 M. The anolyte was a 0.5 M borate buffer solution (pH 9.2) with 0.5 M sodium sulfite. All potentials were reported vs SCE and RHE (V vs RHE = V vs SCE + 0.244V + 0.0591pH). The cell was thermostated with a water bath at 25 °C. The ohmic drop (i$R_u$, i: current density, $R_u$: uncompensated resistance) for all the Linear sweep voltammetries (LSVs) was corrected after measurements, whereas the constant-potential electroreductions were measured without compensation. Note that very low $R_u$ values (ca. 1-2 Ohm) are measured. To avoid the presence of dissolved oxygen, all the solutions were purged with $N_2$ before each electrochemical experiment, and a $N_2$ flow was kept in the open space of the cell during experiments. In the LSVs, the potential was scanned from 0 to −1.4 V vs SCE (from 0.79 to -0.61 V vs RHE) at a scan rate of 1 mV/s in the electrolytes without HMF and 5 mV/s in those with HMF as reported elsewhere [S4]. Electrocatalytic reductions were performed potentiostatically at -0.51 V vs RHE potential. The solution was kept under stirring, with a PTFE coated magnetic bar (15 mm diameter), at 1000 rpm. The catalytic cycle started with a sequence of LSV in borate and borate plus HMF, followed by electrolysis at constant current or potential and then the first two LSVs were repeated. Several cycles could be performed over the same electrocatalyst, either modifying or keeping constant the current or potential applied. The reactions were carried out under total HMF conversion conditions, which were obtained through the transfer of the charge necessary to convert all HMF in solution into BHMF (i.e. through a 2 $e^-$ process) assuming a 100 % Faradaic Efficiency. Some selected reactions were also performed at a short time. At the end, the solutions were collected and analyzed with HPLC. All the measurements were performed in three replicates. The geometric surface areas of the electrodes were considered to determine the current densities.

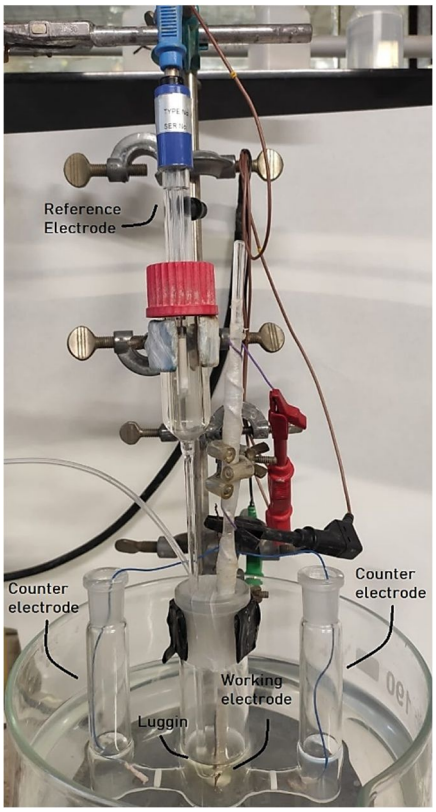


**Electrochemical cell and electrodes used in all the experiments reported in this work**

The double-layer capacitance was determined through CV analysis in a suitable potential window where no redox reactions were occurring, hence no faradic current contributed to the voltammogram. In detail, the cyclic voltammetries were carried out in the potential window between -0.65 and 1.00 V vs SCE (-0.14 and -0.22 V vs RHE), recording five different voltammograms (five cycles each) with a scan rate of 10 mV/s, 20 mV/s, 40 mV/s, 80 mV/s and 150 mV/s, respectively. The double-layer capacitance was determined as the slope of the linear fitting of the difference between the anodic and cathodic capacitive current at 0.825 V vs SCE (-0.04 V vs RHE) vs the scan rate.

An HPLC Agilent 1260 Infinity Series equipped with a Cortecs T3 2.4 µm (4.6 x 100 mm) was used to analyze and quantify the reaction products. The instrument operates at 30 °C, with an autosampler (injection volume 1 µL) and a Diode-Array Detector set at 284 nm for the identification of HMF and 223 nm for the identification of BHMF. The analyses were performed with gradient elution in three steps: isocratic conditions for 6 minutes, with eluent composed of $CH_3CN/H_2O$ 10/90 v/v ratio; gradient elution for 5 minutes until a $CH_3CN/H_2O$ 50/50 elution ratio was obtained; gradient elution for 4 minutes until a $CH_3CN/H_2O$ 70/30 elution ratio was obtained. The flow rate was 0.7 mL $min^{-1}$.

Conversion ($X_{HMF}$), Selectivity ($S_{BHMF}$), Faradaic Efficiency (FE), BHMF productivity and Carbon balance were calculated with the following equations:

$$X_{HMF}(\%) = \frac{mol_{HMF\ consumed}}{mol_{HMF\ initial}} x100$$

$$S_{BHMF}(\%) = \frac{mol_{BHMF\ formed}}{mol_{HMF\ consumed}} x100$$

$$FE\ (\%) = \frac{mol_{BHMF\ formed}}{total\ charge\ passed/(2F)} x100$$

$$BHMF\ productivity = \frac{mmol_{BHMF\ formed}}{reaction\ time\ (h)\ *\ area\ (cm^2)}$$

where F is the Faraday constant. The area corresponds to the geometric area of electrodes, i.e. 2.64 $cm^2$.

### 1.5. Beamline, *in situ e*lectrochemical cell and electrode preparation

Measurements were carried out at the innovative station for in situ spectroscopy (ISISS) beamline at the BESSY II electron storage ring operated by the Helmholtz-Zentrum Berlin für Materialien und Energie [S5]. The photons are sourced from a bending magnet (D41) and a plane grating monochromator (PGM) yielding an energy range from 80 eV to 2000 eV (soft X-ray range), with a flux of $1.4x10^{11}$ photons/s at 900 eV photon energy at 0.1 A ring current using a 111 µm slit and a 80 µm x 200 µm beamspot size. The *in situ* electrochemical cell [S6] is operated with a background pressure of ~$10^{-7}$ mbar while the aqueous electrolyte circulated on the back side of a $Si_3N_4$ membrane. The pristine $Si_3N_4$ membranes (type NX10100C) were sourced from Norcada (Edmonton, Canada). On the $Si_3N_4$ membrane (100 nm thick) a thin film of Cr (3 nm) adherence layer was deposited by physical vapor deposition (PVD). After that, 20 nm of Cu were deposited onto the 3 nm Cr by PVD. We obtained a homogeneous polycrystalline thin film with an X-ray transmission through this membrane of approximately equal to 80%. The covered $Si_3N_4$ membrane are used as working electrodes and X-ray windows at the same time that separates the electrolyte from the vacuum, where the photo-diode detector is placed (AXUV100 Opto Diode Corp). This electrode was used for the electrodeposition Cu and $CeO_2$ electrodes. The diameter of the O-ring (0.7 cm) used for sealing the electrochemical cell determines the effective area of the electrode equal to ~0.38 $cm^2$. The measurements were recorded at cff 1.4 to avoid overlapping contribution of second order Si K-edge (from the $Si_3N_4$ membrane) at around 920 eV. No beam effects were observed during consecutive scans, which rules out detectable beam-damage in the electrodes. The main body of the cell is made of polyether ether ketone (PEEK), which is an electrical insulator and is chemically inert to most of the aqueous electrolytes. The counter electrode is a Pt wire and the reference electrode is a Ag/AgCl FLEXREF, sourced from World precision Instruments (Florida, USA). The electrolyte flow is assured

with a peristaltic pump PERIMAX 16- Antipuls sourced from SPETEC GmbH (Erding, Germany). Potentiometric control during the *in situ* X-ray absorption near-edge structure spectroscopy in total fluorescence yield mode (XANES-TFY) characterization is guaranteed by a potentiostat SP-300, Biologic (Seyssinet-Pariset, France), allowing for different electrochemical characterization modes as cyclic voltammetry (CV), linear sweep voltammetry (LSV) and chronoamperometry (CA).

The electrodes were prepared by electrodeposition onto the PVD copper electrode by:

1) **Cu/Cu deposition:** Solution 0.005 M $CuSO_4 \times 5H_2O$ 99.95% + 0.04 M $H_2SO_4$ 96% in UPW, at -0.255 V vs Ag/AgCl (0.01 V vs RHE) during 200 s.

2) **$CeO_2$/Cu deposition:** 0.15 M $Ce(NO_3)_3 \times 6H_2O$ 99.5% in UPW, at -0.855 V vs Ag/AgCl (-0.36 vs RHE) during 100 s.

Following the electrodeposition condition 1 for Cu/Cu deposition, a couple of in-situ spectra were collected in XANES-TFY mode in open-circuit voltage (OCV), which are labelled as OCV after 4 min and OCV after 12 min in Figure S1a.

A second PVD-Cu sample was used for the $CeO_2$/Cu deposition. First, the EC-cell was flushed with UPW at which a XANES spectrum was collected and labelled as $H_2O$ bef. ED in Figure S1b. Likewise, consecutive XANES spectra were collected in flowing 0.15 M $Ce(NO_3)_3$ before and after electrodeposition, and a last one in flowing UPW (Figure S1b).

Figure S1 shows the Cu L-edge and Ce M-edges of the a) Cu deposition under condition 1 on 20 nm thick PVD Cu, and b) $CeO_2$ on Copper under condition 2. These results indicate that copper is deposited as metallic copper. Moreover, Ce is deposited as $Ce^{4+}$ meanwhile the PVD Cu electrode is partially oxidized to $Cu^{2+}$.

Once the electrodes were electrodeposited the EC-cell was flushed with UPW to eliminate the electrolyte and after that the electrolyte for the electrocatalytic experiments was flowed inside. The electrolytes were the same than those used for the electrocatalytic tests: 0.5 M borate buffer and 0.05 M HMF.

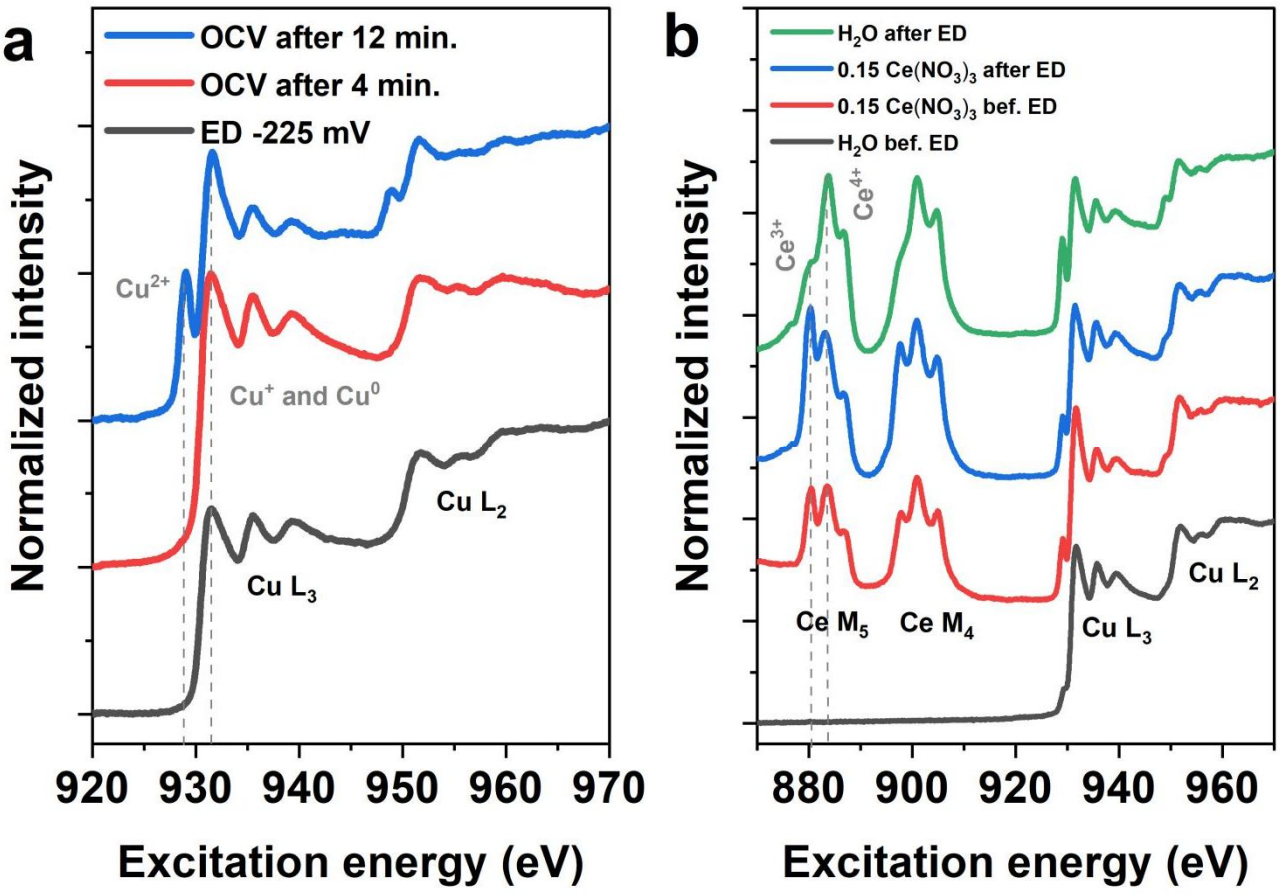


**Figure S1.** In situ XANES-TFY measurements collected of the electrodeposited electrodes on PVD copper: (a) Cu/Cu deposition by condition 1 specified in section 1.5, where OCV measurements are performed after the deposition (b) Ce/Cu deposition by condition 2 specified in section 1.5, where $H_2O$ before ED and 0.15 $Ce(NO_3)_3$ before ED are measured in flowing UPW and 0.15 M $Ce(NO_3)_3$ before the electrodeposition. respectively. Likewise, 0.15 $Ce(NO_3)_3$ after ED and $H_2O$ after ED are respectively measured in flowing 0.15 M $Ce(NO_3)_3$ and UPW after the electrodeposition.

**Table S1.** Summary of the average of deposited mass after electrodeposition conditions and crystallite size of $CeO_2$ for as deposited and spent catalysts.

| **$Ce(NO_3)_3$ conc** | **Electrocatalyst** | **Deposited mass / mg** | **D / nm $CeO_2$(111)** |
|---|---|---|---|
| 0.15 M | As deposited<br>After tests | 52 | 7.4<br>7.7 |
| 0.10 M | As deposited<br>After tests | 105 | 7.5<br>8.0 |

**Figure S2.** Electrocatalytic performance of $CeO_2$/Cu foam in the reduction of 0.02 M HMF to BHMF. Electrodeposition: -0.9 V vs SCE (-0.3605 V vs RHE) for 100 s with a 0.15 M $Ce(NO_3)_3$ electrolyte.

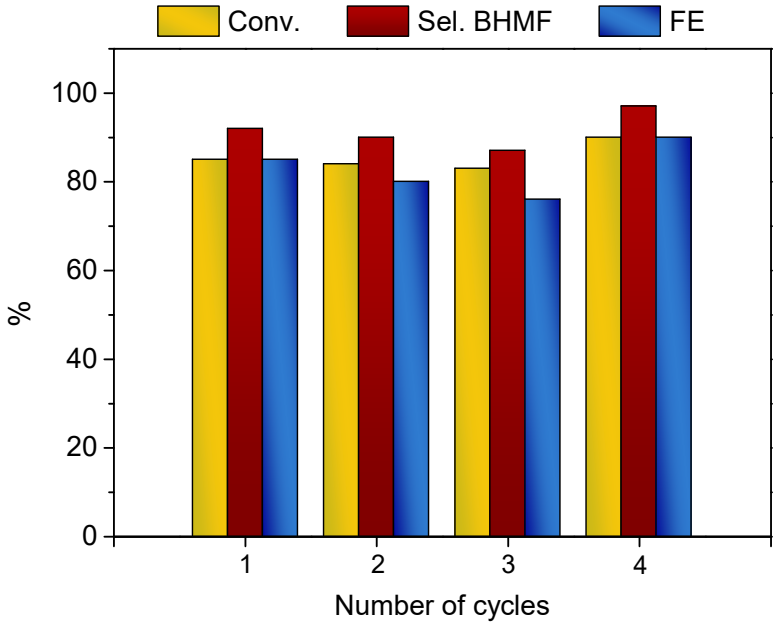


Data were obtained after the tests reported in Figure 3 with the 0.10 M HMF electrolyte. The total reaction time with the same $CeO_2$/Cu foam, including electrolysis with the 0.02, 0.05 and 0.10 M solutions and the LSVs in borate and HMF, was around 25 h.

The differences observed in the results at different cycles are related to the standard deviation of the results rather than to the stability of the catalyst.

The reaction times for cycle depended on the concentration and the activation:

- 0.02 M ca. 1500, 2000 and 2500 s
- 0.05 M ca. 9000 and 9000 s
- 0.10 M ca. 22000 s.
- 0.02 M ca. 5000, 3400, 3100, 5200, 4100 s.

**Figure S3.** Electrocatalytic performance of $CeO_2$/Cu catalysts. a) 0.05 M HMF, average of 6 measurements each with a new electrocatalyst; b) 0.10 M HMF average of 4 measurements each with a new catalyst; c) 0.05 M HMF, three consecutive cycles with the same electrocatalyst. Electrodeposition: -0.9 V vs SCE (-0.3605 vs RHE) for 100 s with a 0.15 M $Ce(NO_3)_3$ electrolyte.

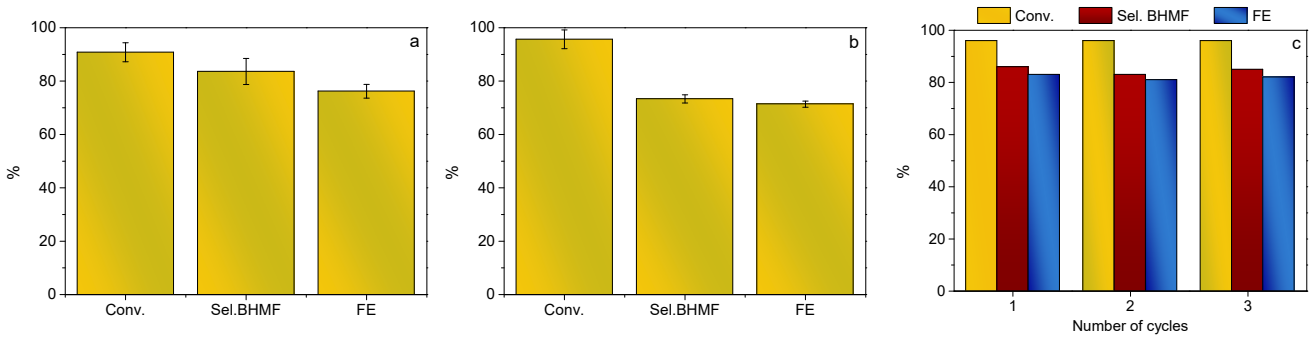


The results in c) show that the performance was similar in three consecutive cycles, indicating that the catalyst was stable.

It should be noted that the differences in the activation time depending on the concentration of the HMF electrolyte (0.02 and 0.05 M) could be related to the current generated. It was larger in the more concentrated electrolyte, hence the reduction and growth of copper could be more promoted.

**Figure S4.** SEM images of an Ag/$CeO_2$/Cu foam after electrocatalytic tests summarized in Table S2 where it is possible to observe the deposition of Ag over the $CeO_2$ coating. a, c) low magnification images; b, d) high magnification images where it is possible observe Ag deposited particles, confirmed by EDS in e).

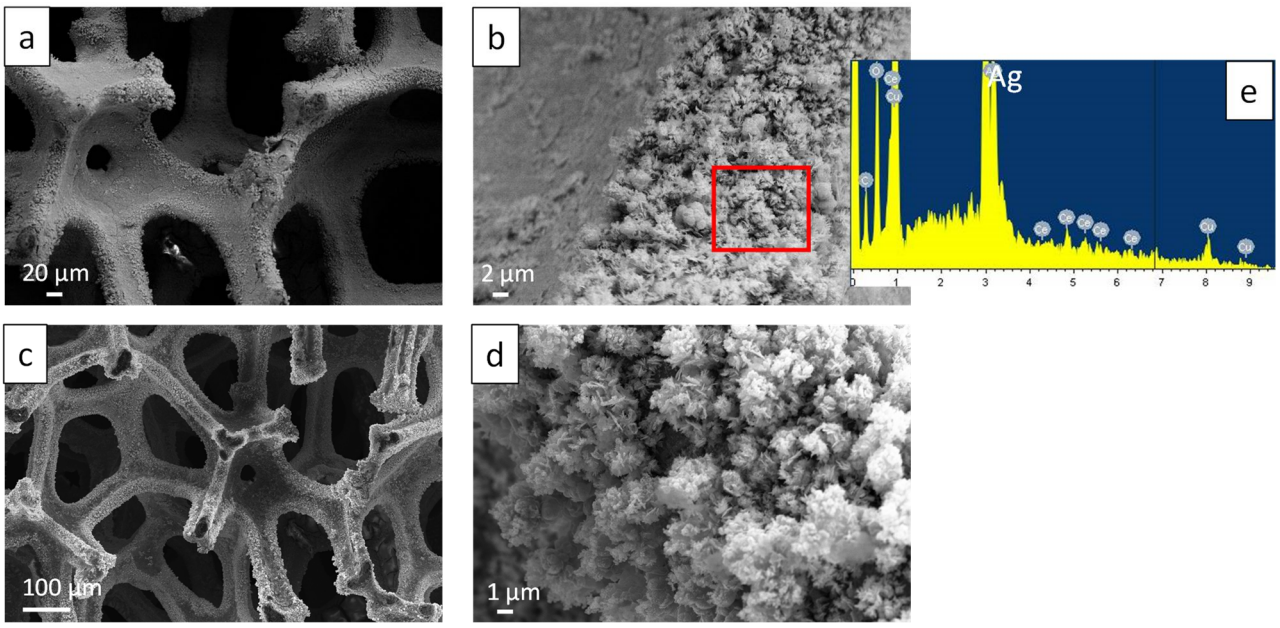


**Table S2.** Electrocatalytic performance of Ag/$CeO_2$/Cu foam in the reduction of HMF to BHMF modifying the HMF concentration in the electrolyte (0.02, 0.05 and 0.10 M HMF). Electrodeposition: -0.9 V vs SCE (-0.3605 vs RHE) for 100 s with a 0.15 M $Ce(NO_3)_3$ electrolyte + $AgNO_3$ 25 s -0.9 V vs SCE.

| Conc. HMF / M | Conv. HMF / % | Sel. BHMF / % | FE / % |
|---|---|---|---|
| 0.02 | 72 | 99 | 74 |
| | 81 | 98 | 82 |
| | 76 | 94 | 74 |
| 0.05 | 98 | 87 | 88 |
| | 98 | 84 | 84 |
| | 98 | 81 | 81 |
| 0.10 | 99 | 65 | 66 |
| 0.02 | 83 | 98 | 79 |

**Figure S5.** Tafel plots obtained in the LSVs shown in Figure 4a and 4b for the $CeO_2$/Cu catalyst in borate a) and 0.05 M HMF electrolytes b).

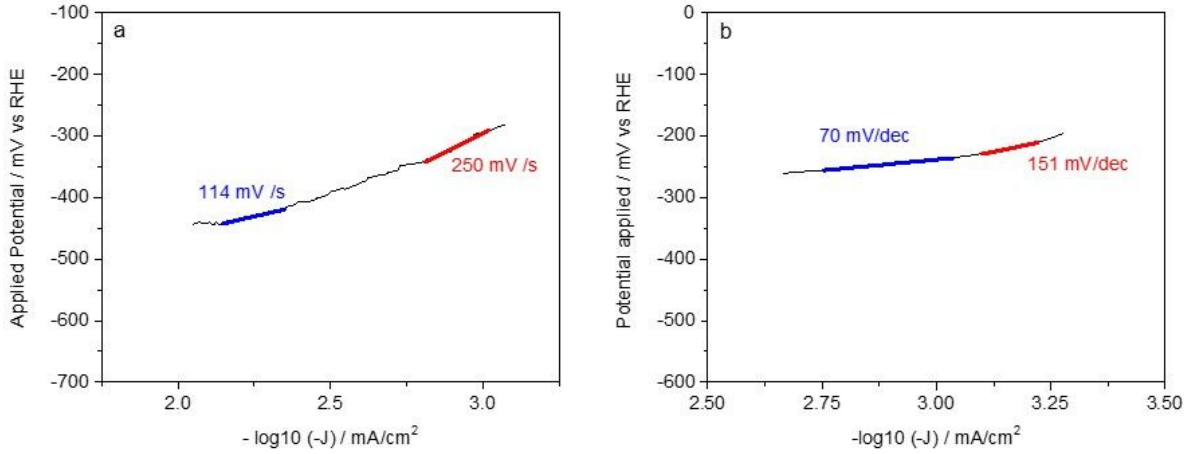


The Tafel slope value in both borate and HMF depends on the potential region where it was calculated. Close to the onset potential rather high values are obtained, i.e. 250 mV/dec in borate and 140 mV/dec in HMF. Instead in a more cathodic potential region, free of mass-transfer limitation, the values decrease to 114 mV/dec in borate and 70 mV/dec in HMF. These values are rather close to those previously reported by us for the AgCu foam catalysts in the same electrolytes [S3]. The differences in the values depending on the potential could be related to changes in the catalyst at the beginning of the discharge, indeed the catalyst could be reduced, $Ce^{4+}$ to $Ce^{3+}$ and $Cu^{2+}$ to $Cu^0$ (confirmed by in situ measurements in this work) these phenomena could decrease the kinetics as previously reported [S7].

**Figure S6.** Evolution of the LSVs in borate and 0.02 M HMF with the electrocatalytic reaction cycles for the $CeO_2$/Cu foam. Electrodeposition: -0.9 V vs SCE (-0.3605 vs RHE) for 100 s with a 0.15 M $Ce(NO_3)_3$ electrolyte.

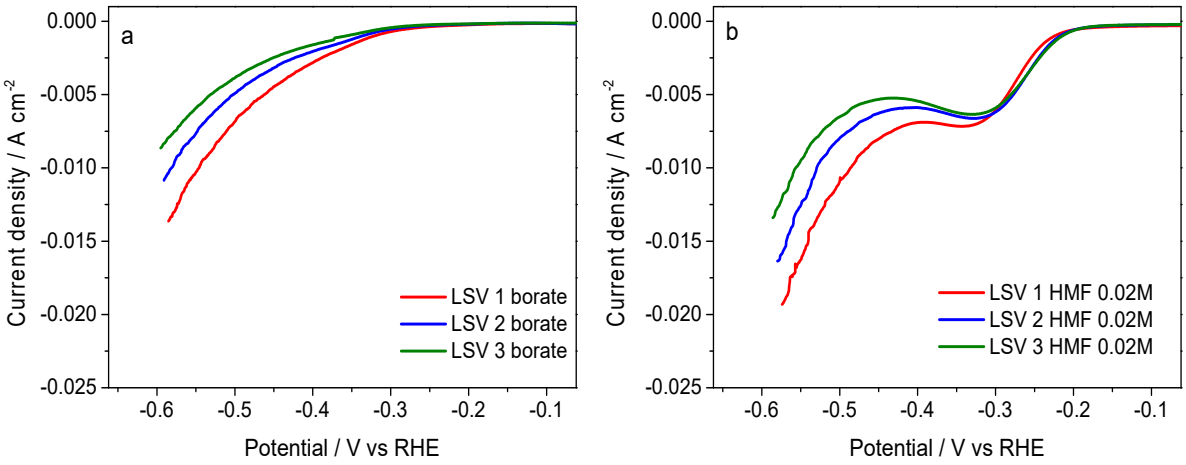

**Figure S7.** a, b) Representative CVs recorded at 5, 10, 20, 40, 80, and 150 mV/s over the Cu bare foam (a) and the $CeO_2$/Cu foam (b) immersed in the borate electrolyte (pre reaction). The Cu bare foam and the $CeO_2$/Cu foam were previously subjected to a LSV in borate. c) linear fitting of the difference between the anodic and cathodic capacitive current -0.04 V vs RHE vs the scan rate. d) values of the double $C_{DL}$ obtained from the slope of the fittings in c).

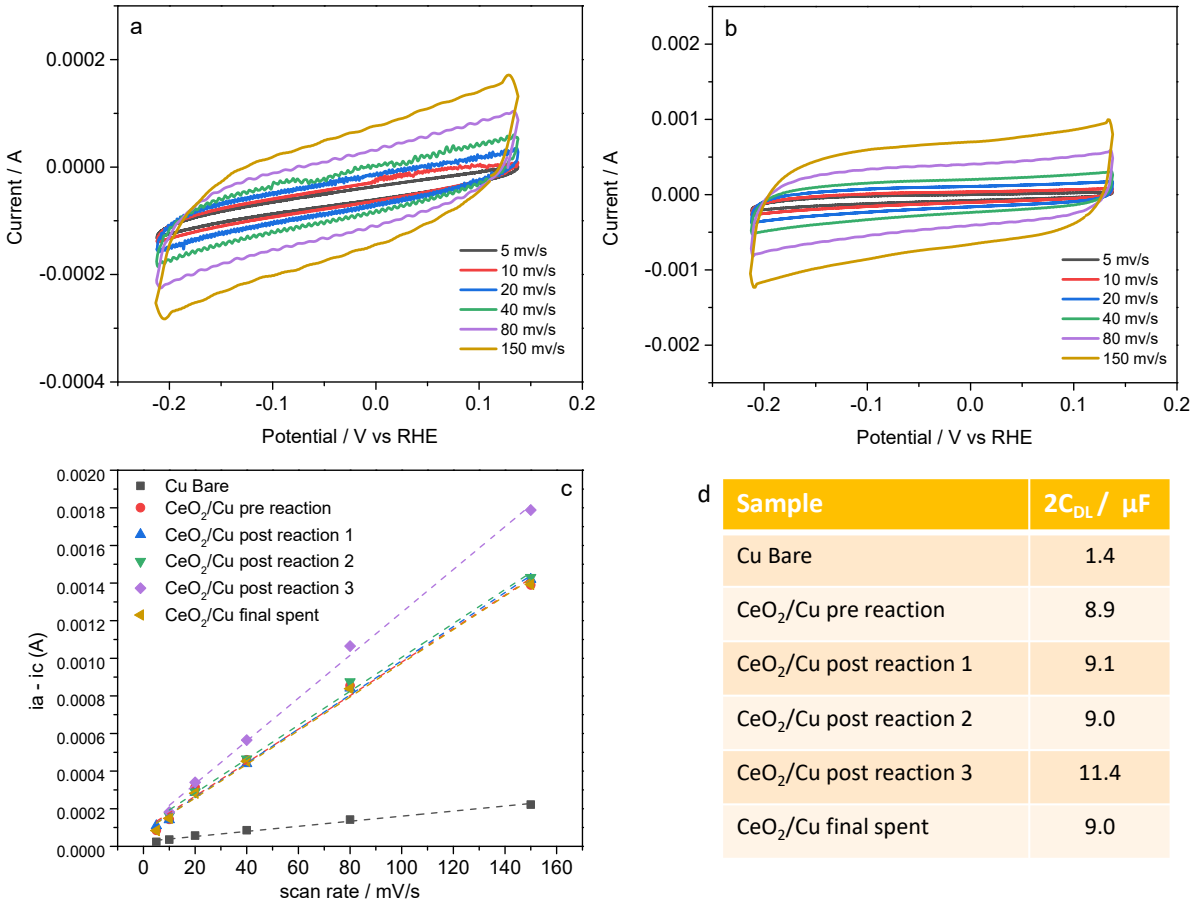


d

| Sample | $2C_{DL}$ / µF |
|---|---|
| Cu Bare | 1.4 |
| $CeO_2$/Cu pre reaction | 8.9 |
| $CeO_2$/Cu post reaction 1 | 9.1 |
| $CeO_2$/Cu post reaction 2 | 9.0 |
| $CeO_2$/Cu post reaction 3 | 11.4 |
| $CeO_2$/Cu final spent | 9.0 |

The measurements were performed over the same $CeO_2$/Cu catalyst subjected to the following conditions:

- $CeO_2$/Cu pre reaction: after the 1st LSV in borate
- $CeO_2$/Cu post reaction 1: after the 1st electroreduction of a 0.05 M HMF electrolyte.
- $CeO_2$/Cu post reaction 2: after the 2nd electroreduction of a 0.05 M HMF electrolyte.
- $CeO_2$/Cu post reaction 3: after the 3rd electroreduction of a 0.05 M HMF electrolyte.
- $CeO_2$/Cu spent: after the 3rd electroreduction of a 0.05 M HMF electrolyte and washing with water and acetonitrile.

**Figure S8.** SEM image of the $CeO_2$/Cu catalyst (0.15 M $Ce(NO_3)_3$; -0.9 V vs SCE (-0.3605 vs RHE) for 100 s) after electrocatalytic tests where some coating detachment can be observed. The catalyst was tested for ca. 25 h in the reaction conditions reported in Figure 3 and Figure S2 with all the three 0.02, 0.05 and 0.10 M HMF electrolytes (including LSVs in borate and HMF).

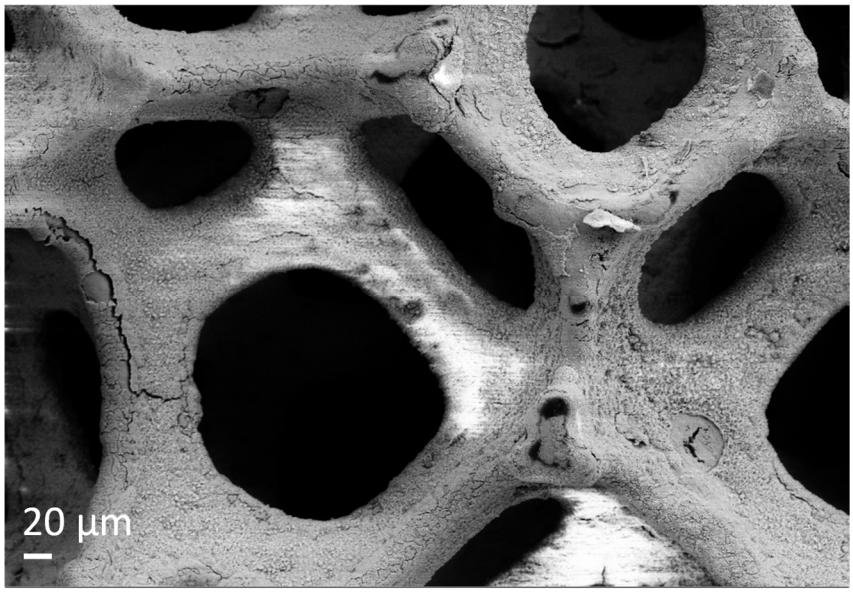

**Figure S9.** SEM/EDS characterization of $CeO_2$/Cu foam electrodeposited at -0.9 V vs SCE (-0.3605 vs RHE) for 100 s with the 0.15 M $Ce(NO_3)_3$ electrolyte after electroreduction. a-c) Secondary electron images at different magnification; d) Backscattering image corresponding to the zone investigated in c. EDS spectra of the regions of interest indicated in image c). The spent catalyst was tested for ca. 25 h in the reaction conditions reported in Figure 3 and Figure S2 with all the three 0.02, 0.05 and 0.10 M HMF electrolytes (including LSVs in borate and HMF).

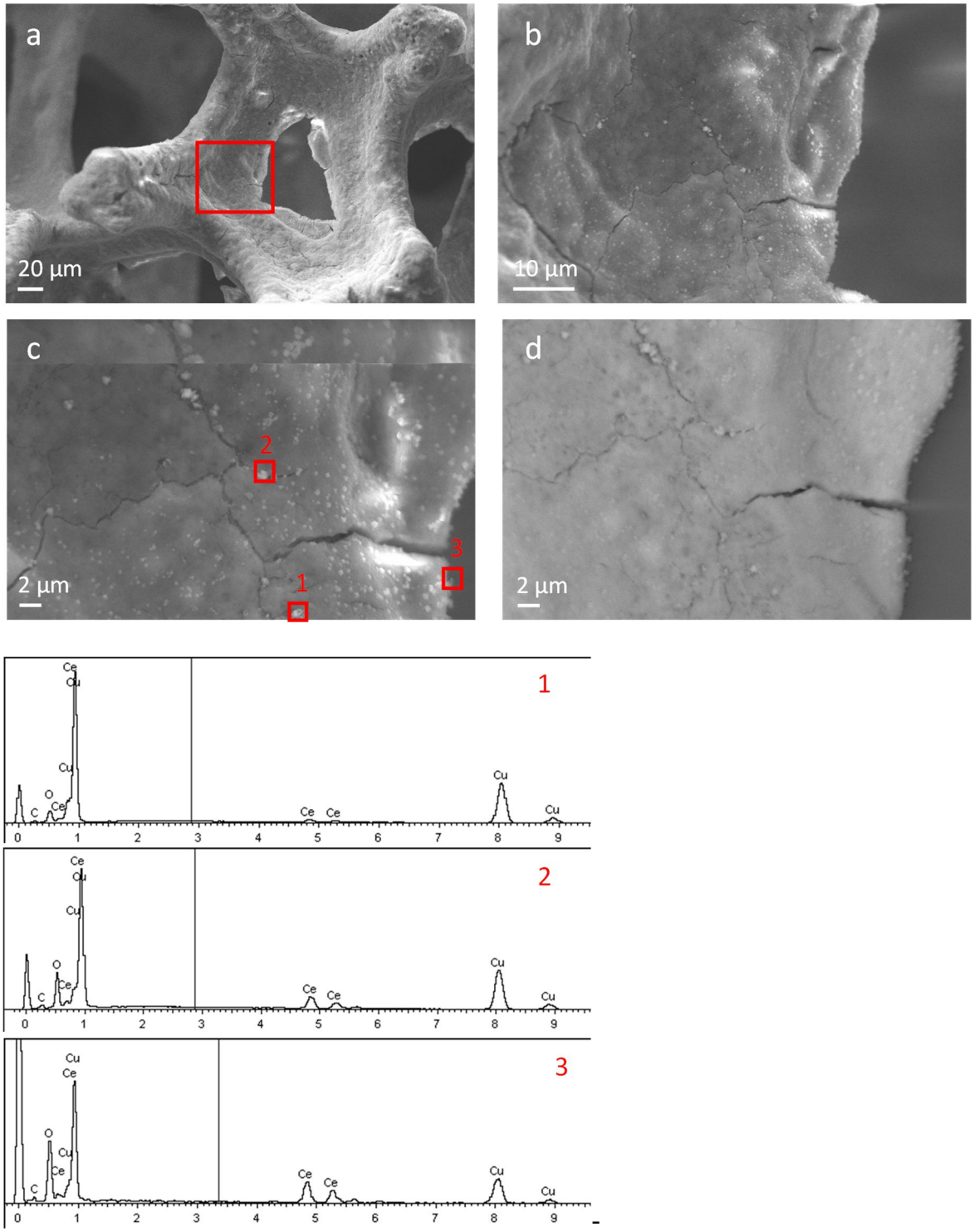

**Figure S10.** HRTEM characterization of a spent coating prepared with a 0.15 M $Ce(NO_3)_3$ electrolyte at -0.9 V vs SCE (-0.3605 vs RHE) for 100 s: a-d). HRTEM images at different magnifications where Cu nanoparticles (black dots) on the $CeO_2$ were observed, SAED were obtained in figure d; e) HAADF image, the EDS spectrum was recorded along the yellow line. The spent catalyst was tested for ca. 25 h in the reaction conditions reported in Figure 3 and Figure S2 with all the three 0.02, 0.05 and 0.10 M HMF electrolytes (including LSVs in borate and HMF).

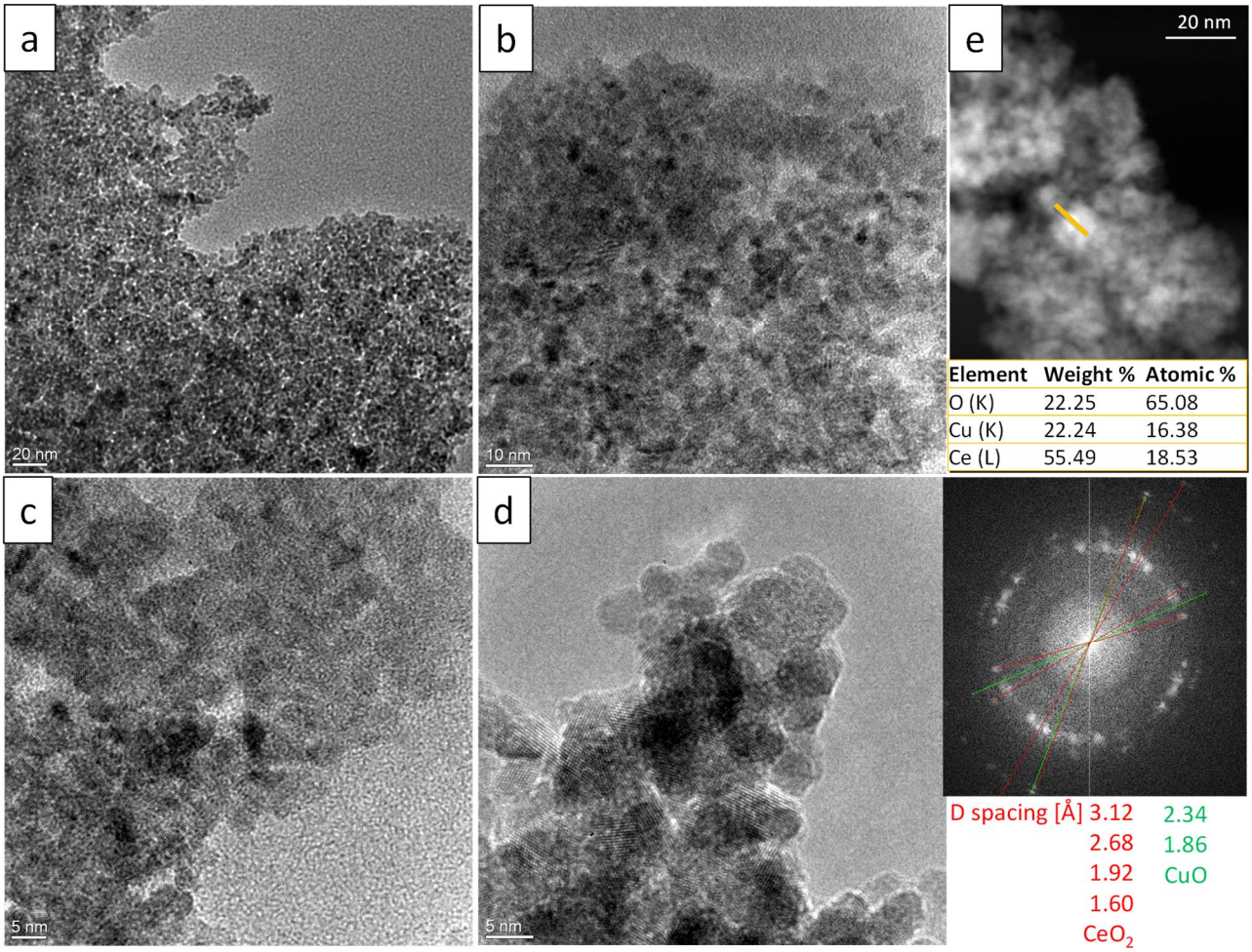

**Figure S11.** Electrocatalytic activity of a Cu bare foam and of a foam treated in 0.1 M $KNO_3$ at -1.1 V vs SCE (-0.5605 vs RHE) for 100 s.

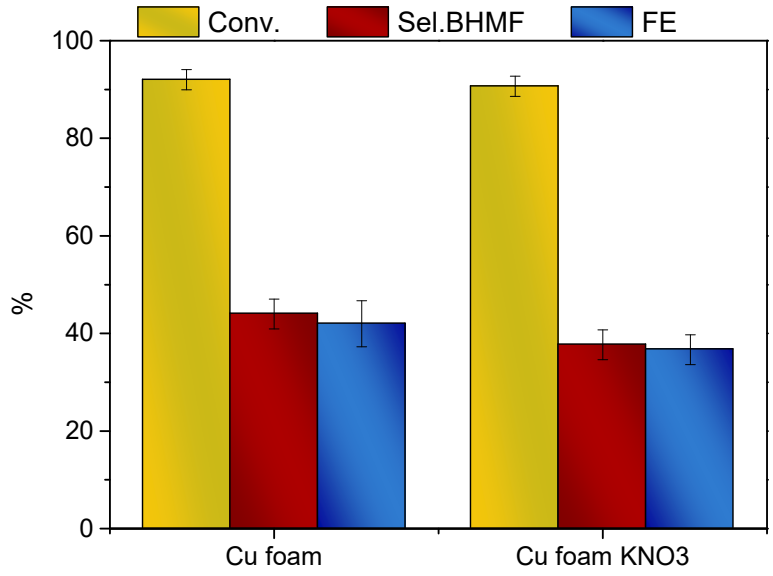

**Figure S12.** Characterization of the thick coating ($CeO_2$/Cu 0.10) prepared with a 0.10 M $Ce(NO_3)_3$ electrolyte at -1.1 V vs SCE (-0.5605 vs RHE) for 200 s. (a) SEM image; (b) diffraction pattern and (c) micro-Raman spectra of as deposited and spent catalysts. For comparison purposes the characterization of thin coating ($CeO_2$/Cu 0.15) is added. The spent catalyst was tested for ca. 7 h with the 0.10 M HMF electrolyte (including LSVs in borate and HMF).

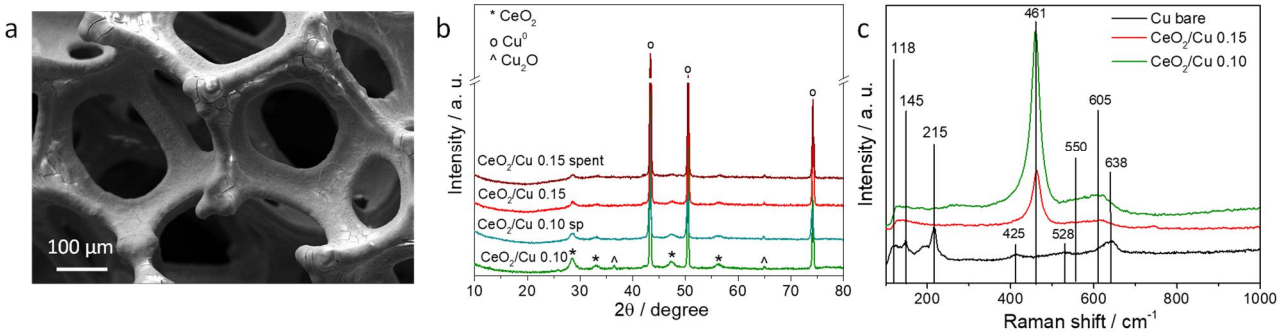

**Figure S13.** Effect of the thickness of the $CeO_2$ coating on the LSV in borate electrolyte (a), in borate + 0.10 M HMF electrolyte (b) and on the catalytic performance, 0.10 M HMF -0.51 V vs RHE (c). Thin = $CeO_2$/Cu 0.15; Thick = $CeO_2$/Cu 0.10.

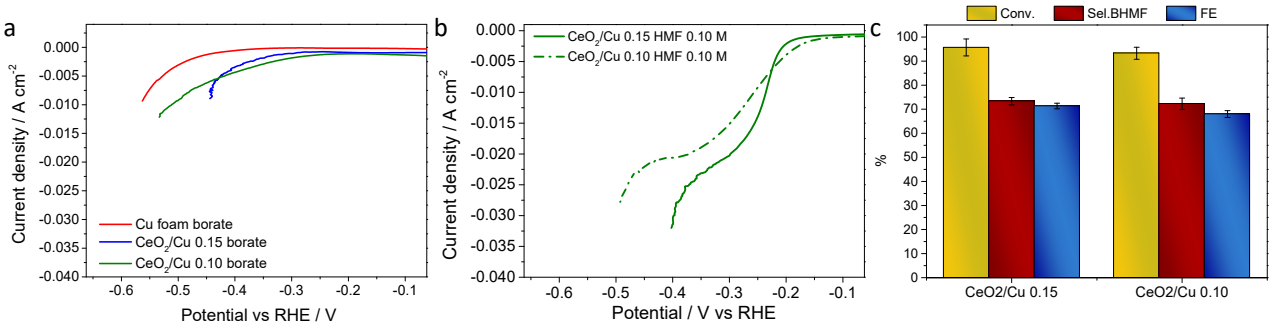

**Figure S14.** SEM images of the spent electrocatalyst (thick layer) synthesized at -1.1 V vs SCE (-0.5605 vs RHE), 0.10 M $Ce(NO_3)_3$, and 200 s. a) low magnification image to observe the stability of the coating; b-d) high magnification images where it is possible to observe the copper particles, the EDS in the inset of b shows the composition of the coating in the image. The spent catalyst was tested for ca. 7 h with the 0.10 M HMF electrolyte (including LSVs in borate and HMF).

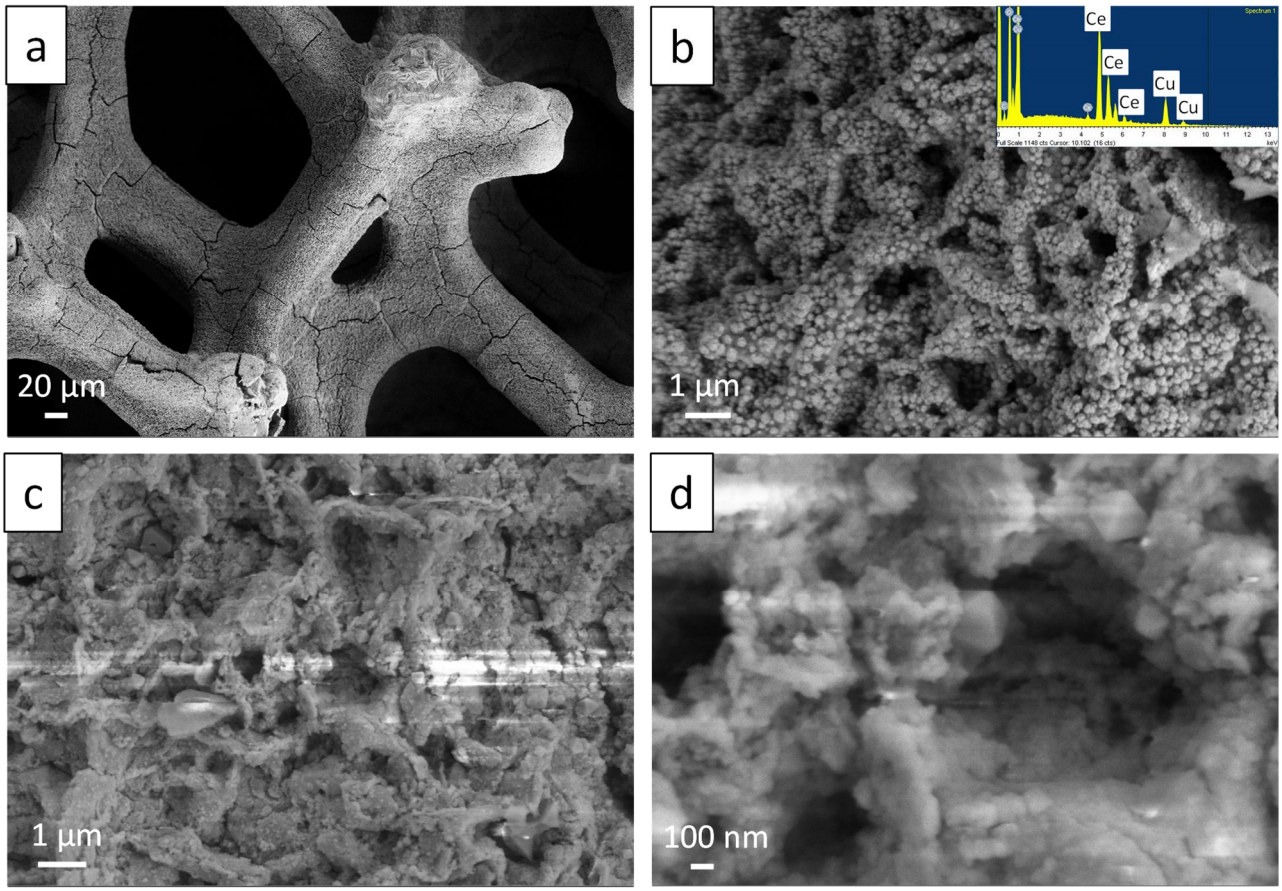

**Figure S15.** Representative SEM images of a spent coating after: a) the first LSV in borate; b) two cycles of tests with the 0.05 M HMF electrolyte: c) cycles with all the three 0.02 M, 0.05 M and 0.10 M electrolytes. Electrodeposition conditions: -0.9 V vs SCE (-0.3605 vs RHE) for 100 s with the 0.15 M $Ce(NO_3)_3$ electrolyte

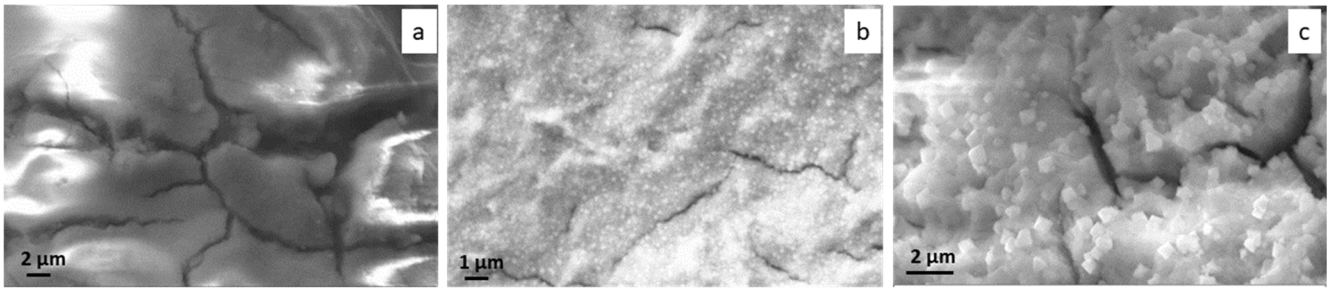

**Figure S16.** SEM images at different magnification (a-c) of an Ag foam coated by $CeO_2$. Electrodeposition conditions: 0.15 M $Ce(NO_3)_3$ electrolyte, -0.9 V vs SCE (-0.3605 vs RHE) for 100 s.

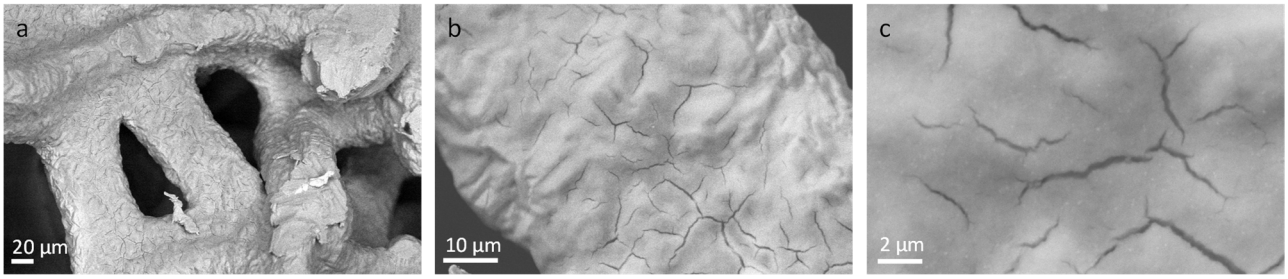

**REFERENCES**

(S1) Ho, P. H.; Ambrosetti, M.; Groppi, G.; Tronconi, E.; Fornasari, G.; Vaccari, A.; Benito, P. Electrodeposition of $CeO_2$ and Pd-$CeO_2$ on small pore size metallic foams: Selection of deposition parameters, *Catal. Today* **2019**, *334*, 37-47.

(S2) Montante, G.; Carletti, C.; Maluta, F.; Paglianti, A. Solid dissolution and liquid mixing in turbulent stirred tanks, *Chem. Eng. Technol.* **2019**, *42*, 1627–1634.

(S3) Sanghez de Luna, G.; Ho, P. H.; Sacco, A.; Hernández, S.; Velasco-Vélez, J.-J.; Ospitali, F.; Paglianti, A.; Albonetti, S.; Fornasari, G.; Benito, P. AgCu Bimetallic Electrocatalysts for the Reduction of Biomass-Derived Compounds, *ACS Appl. Mater. Interfaces* **2021**, *13*, 23675–23688.

(S4) Sanghez de Luna, G.; Ho, P. H.; Lolli, A.; Ospitali, F; Albonetti, S.; Fornasari, G.; Benito, P. Ag Electrodeposited on Cu Open-Cell Foams for the Selective Electroreduction of 5-Hydroxymethylfurfural, *ChemElectroChem* **2020**, *7*, 1238– 1247.

(S5) https://www.helmholtz-berlin.de/pubbin/igama_output?modus=einzel&gid=1671]

(S6) Velasco-Velez, J.-J.; Mom, R. V.; Sandoval-Diaz, L.-E.; Falling, L. J.; Chuang, C.-H.; Gao, D.; Jones, T. E.; Zhu, Q.; Arrigo, R.; Roldan Cuenya, B.; Knop-Gericke, A.; Lunkenbein, T.; Schlögl, R. Revealing the Active Phase of Copper during the Electroreduction of $CO_2$ in Aqueous Electrolyte by Correlating In Situ X-ray Spectroscopy and In Situ Electron Microscopy, *ACS Energy Lett.* **2020**, *5*, 2106−2111.

(S7) Valenti, G.; Melchionna, M.; Montini, T.; Boni, A.; Nasi, L.; Fonda, E.; Criado, A.; Zitolo, A.; Voci, S.; Bertoni, G.; Bonchio, M.; Fornasiero, P.; Paolucci, F.; Prato, M. Water-Mediated ElectroHydrogenation of $CO_2$ at Near-Equilibrium Potential by Carbon Nanotubes/Cerium Dioxide Nanohybrids, *ACS Appl. Energy Mater.* **2020**, *3*, 8509−8518.